



THE CLAW SIGN'S DIAGNOSTIC USEFULNESS IN PEDIATRIC RETROPERITONEAL TUMORS ON MAGNETIC RESONANCE IMAGING

¹Dr Kailash, ²Dr Sumera Mahar, ³Marya Hameed, ⁴Dr Bhagwan Das, ⁵Dr Abdul Majeed Khan, ⁶Khushboo Chandio

¹MBBS, FCPS (Radiology) Consultant Radiologist SMBB Institute of Trauma CHK Karachi, drkailash31@gamil.com

²Consultant Radiologist. National institute of Rehabilitation medicine (NIRM) hospital Islamabad, drsumeramahra@yahoo.com

³Head of Radiology department, National Institute of child health/JSMU Karachi, dr mash84@gamil.com

⁴MBBS, FCPS (Radiology), Assistant Professor and Head Radiology Department CMCH @ SMBBMU Larkana, drbd32@gmail.com

⁵Assistant Professor Radiology, Mohtarma Benazir Bhutto Shaheed Medical College Mirpur AJK/ DHQ Teaching Hospital Mirpur AJK, drmajeed19@gmail.com

⁶Lecturer, Peoples Nursing School LUMHS Jamshoro, chandiokhushboo786@gmail.com

1073

ABSTRACT:

BACKGROUND: It is recommended that the claw sign be used to distinguish between tumors with renal origin and those without. Magnetic resonance imaging (MRI) claw sign accuracy is uncertain, and it may be hampered by poorer spatial resolution and greater tumor masses upon presentation in impoverished nations.

OBJECTIVE: The objective of this study was to define and assess the claw sign's ability to distinguish renal from non-renal retroperitoneal tumors in young patients undergoing MRI.

METHODS: The claw sign definition was put out. To evaluate the diagnostic accuracies, and inter- and intra-observer reliability, 53 children's magnetic resonance imaging (MRI) examinations, and medical and lab data were examined. Three features of the kidney-tumor interface, which are part of the claw sign, were put to the test: (1) absence of kidney infoldings, (2) smooth, tapering kidney border blending into the tumor, (3) acute superficial angle.

RESULTS: The claw sign's specificity value was 97%, sensitivity= 74%, negative predictive value= 83%, and positive predictive = 94%. The first reader's intra-rater reliability score was 0.72 with a 95% confidence interval and confidence interval range from 0.54 to 0.86, while the second reader was 0.83 with a CI of 95% range from 0.66 to 1.00. For the second reading, the inter-rater reliability Cohen's kappa values were 0.67 with a CI of 95% range of (0.50-0.85) and 0.65 (0.44-0.86), respectively (p-value = 0.0001).

CONCLUSIONS: The three tumor-mass interface traits under investigation are all significant claw sign traits. For all claw sign features and the overall impression, both intra- and inter-rater reliability ranges from modest to high. As a result, albeit lacking in specificity, the claw sign is sensitive in accurately localizing an intra-renal tumor.

KEYWORDS: radiology, pediatrics, radiodiagnosis

eISSN1303-5150

www.neuroquantology.com



INTRODUCTION: With 600–700 new cases recorded annually over the previous 25 years worldwide, childhood cancer is an uncommon disease. (1) The majority of pediatric abdominal tumors have retroperitoneal origins. (2-4) Nephroblastoma, a cancer of the kidneys, and neuroblastoma, typically an extra-renal retroperitoneal cancer, are potentially curable diseases, but their overall survival rates are lower than those reported in developed nations due to their frequent advanced stage of presentation. (5,6) In the evaluation and treatment of a kid who presents with an abdominal tumor, imaging is crucial. Since various cancers have distinct therapeutic care approaches and prognoses, a precise diagnosis is essential. Identifying the tumor's renal or extra-renal origin is a critical step in reducing the differential diagnosis. (7,8) This distinction is not often immediately obvious, especially when dealing with enormous volumes. The source of the claw sign is unclear, and it is often recommended to utilize other discoveries and the lack of a claw sign as a predictor to identify the provenance of a mass. Additionally, there is a lack of clarity in earlier stories, which may cause difficulty in interpretation and may add to the scant proof of the diagnosis's accuracy. There is no guidance on the best imaging techniques, imaging planes, or if the signal should appear on a single tumor-kidney contact or on many for it to be classified as positive.

The presence of a tumor surrounded by a rim of renal parenchyma that resembles a claw is regarded as the lobster claw sign. The kidney border is smooth and tapers constantly with the tumor, and there are no rounding or infoldings of the kidney. These three features are typical of the tumor-mass interface. If the claw sign is present, the mass likely has a renal origin; if it's absent, it probably doesn't.

It is unknown how size affects the claw sign's accuracy. It seems to reason that smaller tumours with more intact renal architecture

would have more accurate claw signs. Unfortunately, children's retroperitoneal tumors typically show as big masses. (10) Larger tumors typically result in significant anatomic deformation, making it difficult to evaluate the tumor-kidney contact critically. This could reduce the precision and application of claw signs. (11,12)

When staging abdominally, both computed tomography (CT) and magnetic resonance imaging (MRI) are equally useful. (13-16) In line with global trends, MRI is favored over CT for guiding surgical decision-making and risk classification in children coming to our institution with retroperitoneal tumors. Concerns about the onset of cancer in young people, who are more sensitive than adults to radiation's confounding factors, as well as the enhanced soft tissue contrast of MRI, are the driving forces behind this. However, the lower spatial resolution of MRI compared to CT may have a diagnostic drawback, which might reduce the precision of findings like the claw sign. The effectiveness of the MRI claw sign as a diagnostic tool has not been studied. Even if the claw sign is considered in concurrence with other signals, radiologists can still assign it undue weight, which might lead to misdiagnoses. A bias might also exist, favoring reporting on positive claw signals while ignoring reporting on negative claw indications.

In this study, we provide an accurate description of the claw sign, assess its correctness, and determine the level of intra- and inter-observer agreement as well as the claw sign's diagnostic performance on MRI. In order to evaluate the claw sign's use and diagnostic efficacy, we routinely inspect local practitioners.

METHODS:

STUDY SETUP AND DESIGN: This retrospective, descriptive research evaluated the intra- and inter-rater consistency and investigative adequacy of the claw sign on the abdomen MRI



at Mayo Hospital, Lahore. It also looked into the occurrence and correctness of the claw sign. The investigation was conducted at the Mayo Hospital in Lahore, Pakistan, in the Division of Radiodiagnosis.

The research included all kids aged 0 to 12 with solid or mixed solid-cystic retroperitoneal tumors who had their first MRI between July 1, 2018, and June 30, 2022. Excluded cases were those with unclear medical, surgical, or laboratory records as well as those without a definitive clinical diagnosis.

DATA COLLECTION & INTERPRETATION: To find every incident that may have been reached within the designated time period at the Mayo hospital were examined. The subgroup of individuals with a tumor that was irrevocably connected to their kidneys was found using the relevant referral paperwork and radiological information. In order to find radiological information explaining the claw sign, the word "claw" was utilized in an automated method of the report.

Two radiologists evaluated the claw sign in the MRI scans of the study population, one who had more than fifteen years of experience and the other a capable fifth-year student who had completed the specialized exams. Neither the referral data nor the first radiographic result was made available to the radiologists. According to previous research, the axial and coronal T2-weighted, gradient echo, and true fast imaging with relatively stable spontaneous inversion (TRUFI) pictures provided the greatest description of the kidney-tumor interface (repetition time [TR] 5 ms, time to echo [TE] 2.5 ms, slice thickness 5 mm). A second interpretation of the pictures was created a month later. To reconcile the discrepancies in the reports, an agreement was achieved.

data analysis

The data was entered into a Microsoft Excel spreadsheet. Variables that were noticed were age, tissue diagnosis, tapering or infolded

kidney edges, obtuse external kidney-tumor angles, axial and coronal tumor sizes, and the presence or absence of the claw sign.

For analysis, the excel data were loaded into SPSS version 26. By cross-tabulating, the binary index variables with the widely accepted histology, the binary index's sensitivity, specificity, and positive and negative predictive values were calculated. The sample estimates' 95% confidence intervals (CI) were given. The effectiveness of axial and coronal tumor dimensions in foretelling the gold standard histology was examined using receiver operating characteristic (ROC) curves. The area below the curve and its 95% confidence intervals were reported.

Both inter- and intra-rater reliability were determined using Cohen's kappa statistics. Dependability greater than what would have happened by chance alone was indicated by a p-value of 0.05.

RESULTS: 53 instances in all, including 31 female patients and 22 male patients, were found. The ages of participants in the research ranged from 1 to 108 months (mean = 30 months, median = 24). In comparison to the mean axial tumor dimension, the median tumor size was 10.0 cm. The mean tumor size was 11.0 cm, whereas 11.4 cm was the median tumor size.

31 (58.5%) of the 53 cases examined were extra-renal tumors, while 22 (41.5%) were intra-renal tumors (Figure 1). Nephroblastoma, mesoblasticnephroma, a localized infective process, a cystic benign teratoma, and nephroblastoma (total of 27) were the intra-renal tumors The extra-renal tumors included neuroblastomas (13) rhabdomyosarcomas (2) adrenal carcinoma (2) phaeochromocytoma (1) adrenal mature cystic teratoma (1), hepatoblastoma (1) paraganglioma (1), and tiny round blue cell tumor (1), Burkitt's lymphoma (1) (Table 1) (Figure 1).

Table 1: Total number of cases

S.no	Case	Numbers
1	Nephroblastoma	27



2	Neuroblastoma	13
3	Mesoblastic nephroma	2
4	Adrenal carcinoma	2
5	Adrenal mature cystic teratoma	1
6	Burkitt lymphoma	1
7	Focal infective process	1
8	Hepatoblastoma	1
9	Small round blue cell tumor	1
10	Rhabdomyosarcoma	1
11	Pheochromocytoma	1
12	Cystic benign teratoma	1
13	Paraganglioma	1
	Total	53

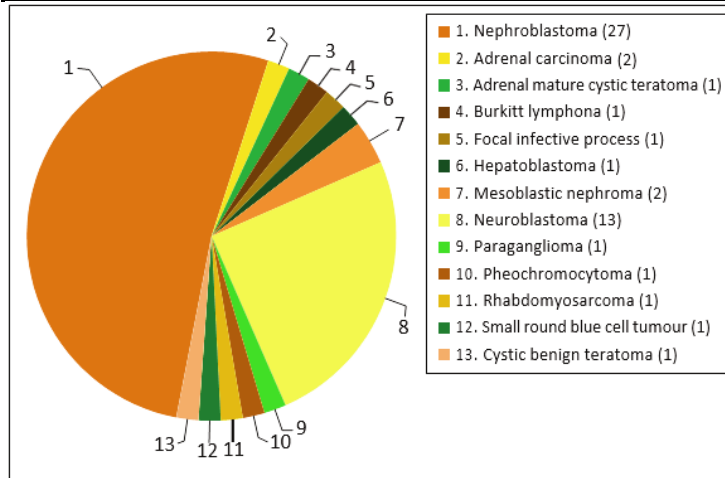


FIGURE 1: Histological frequency (numbers) of the study population.

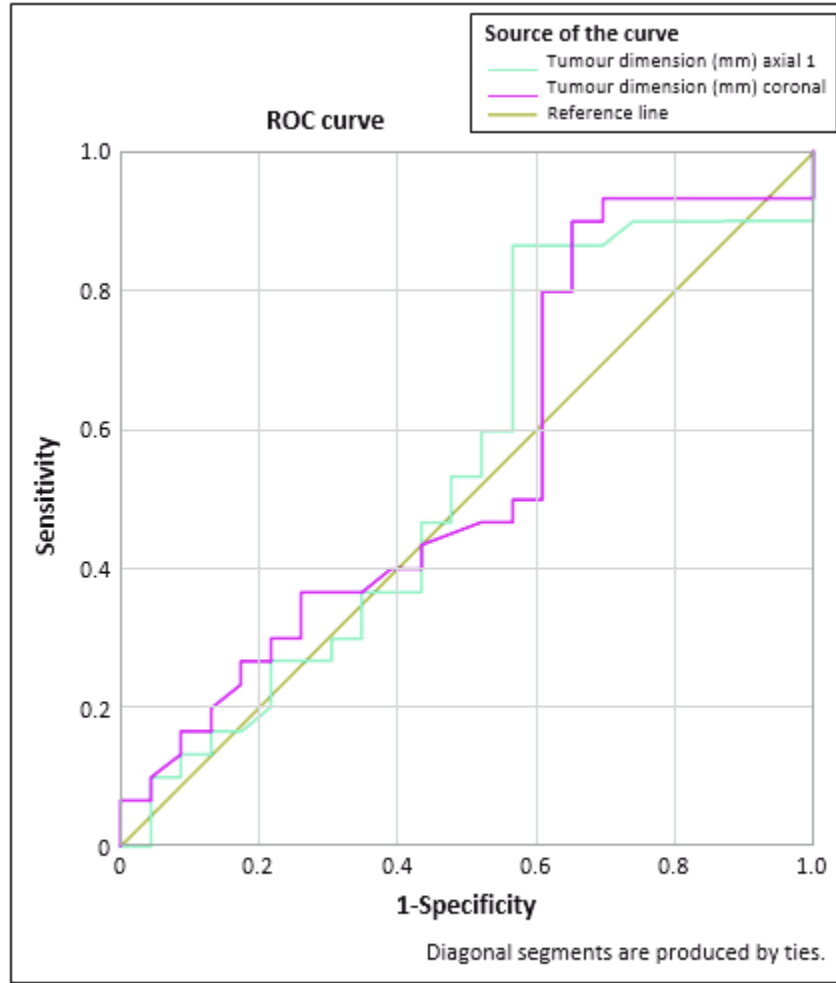


FIGURE 2: Receiver operating characteristic curve of tumour dimensions on coronal and axial magnetic resonance imaging. ROC, receiver operating characteristic.

To evaluate the features of the tumor-mass interface and the claw sign overall, Table 2 includes the specificity, sensitivity, negative and positive predictive values, as well as the intra- and inter-rater reliabilities. The axial tumor diameter on MRI was used as a quantitative

variable, and the ROC analysis result was 0.549, with a 95% confidence range spanning from 0.386 to 0.712. On MRI, the coronal tumour dimension's area under the curve was 0.554 (95% confidence interval: 0.393-0.716). (Figure 2).

Table 2: Summary table of test results

Tumour–mass interface characteristics	Claw sign	Obtuse external interface	Absent infolding	Tapered kidney edge
Negative predictive value (%)	94	89	94	94
Positive predictive value (%)	83	82	81	83
Specificity	74	74	70	74
Sensitivity	97	93	97	97



Intra-rater reliability (first reader) *	Cohen's kappa (95%) (CI)	0.72(0.54–0.86)	0.74(0.56–0.89)	0.71(0.54–0.89)	0.67(0.49–0.85)
Intra-rater reliability (second reader) *		0.83(0.66–1.00)	0.96(0.87–1.00)	0.96(0.87–1.00)	0.96(0.87–1.00)
Inter-rater reliability (first reading) *		0.67(0.50–0.85)	0.69(0.49–0.88)	0.71(0.53–0.86)	0.73(0.53–0.88)
Inter-rater reliability (second reading) *		0.65(0.44–0.86)	0.71(0.52–0.91)	0.83(0.67–0.99)	0.75(0.56–0.94)

*, $p < 0.0001$

DISCUSSIONS: Few, if any, past studies addressing the use and diagnostic effectiveness of the MRI claw sign are known to us. It is sometimes advised to use the claw sign to determine if cancers have extra-renal or renal origins.

With histological correlation serving as the gold standard, the claw sign on an MRI scan in our study population was shown to be a reliable predictor of location with high positive predictive value (94%) and sensitivity (97%) but average specificity (74%) and negative predictive value (83%). The reduced specificity may be explained by the authors' prediction that the usage of the claw sign would become less reliable as tumor size rose.

Palpable abdominal masses were the most frequent clinical manifestation in these individuals, indicating a medium to large tumor size at diagnosis. (17) Kidney anatomy is prone to distortion in large-mass lesions, making it challenging to interpret the claw sign. As previously stated, there is no guidance on the appropriate imaging methods or imaging planes for evaluating the claw sign or regarding whether the manifestation must be visible on a single tumor-kidney interface or multiple for it to be declared positive. Due to the fact that the average tumor size in our sample (9.8 cm) was comparable to the value of 9.82 cm reported in prior research, (18) this finding raises the possibility that the issue of high tumor sizes upon presentation may not be unique to the Pakistan setting.

The ROC analysis showed that the areas under the curves for the axial and coronal tumor diameters were both modest (0.549 and 0.544,

respectively). Due to the poor performance of both quantitative variables, there isn't a suggested anatomical plane for evaluating the claw sign. The appropriate size for the claw symbol's functionality wasn't determined either. This may be influenced by the research population's limitations, translation reliance, or unrecognized reporting bias.

The following three characteristics were taken into consideration in order to make the final diagnosis of a positive claw sign: a renal mass with a tapering renal edge, the lack of infoldings of the kidney edge, and an acute external kidney-tumor interface. There was a considerable degree of intra-rater reliability for each of these signals, with Cohen's kappa values of 0.67, 0.71, and 0.74 for reader one and 0.67, 0.71, and 0.74 for reader two, respectively (0.96 for all three). A very high degree of consensus was revealed by the first read's great inter-rater reliability (0.73, 0.71, and 0.69) and the second read's startlingly similar inter-rater reliability (0.75, 0.83, and 0.71, Table 2).

The different negative and positive claw signs are shown in Figures 3 and 4, respectively. But sometimes, particularly if the tumour is big, imaging data might be conflicting. In this situation, all three signals may not exist simultaneously or may even be in conflict with each other (Figure 5). In this experiment, when there were discrepancies between the imaging results from the axial and coronal scans, it was chosen to give the presence of a tapering renal edge in any plane a positive claw sign. The greatest overall sensitivity (97%), specificity (74%), positive predictive value (83%), and



negative predictive value (94%) were shown by this particular indication.

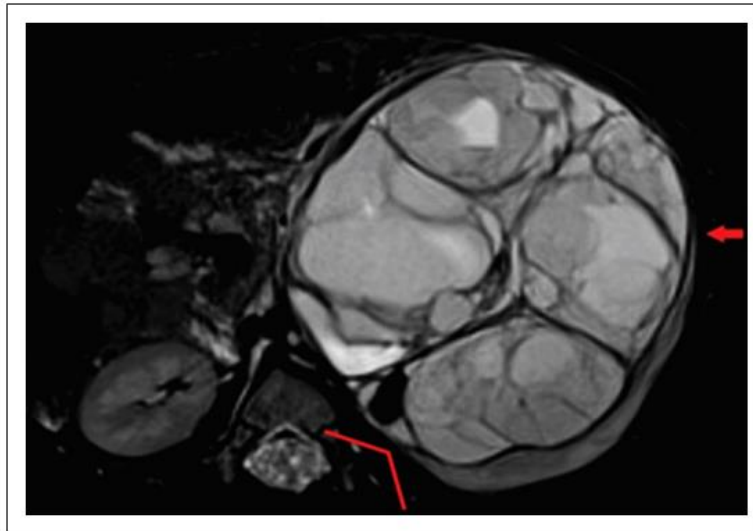


FIGURE 3: Axial fat-suppressed T2-weighted magnetic resonance image of a large cystic nephroblastoma arising from the left kidney. The claw sign is positive with tapering (red arrow), absent infolding and obtuse external kidney–tumour interface (red marker).

1079

As a result, the following is the concise description of the claw sign offered: The claw sign may be considered positive when a renal

mass has a tapering kidney edge that is supported by missing infoldings of the renal edge and a direct outside kidney-tumor contact.

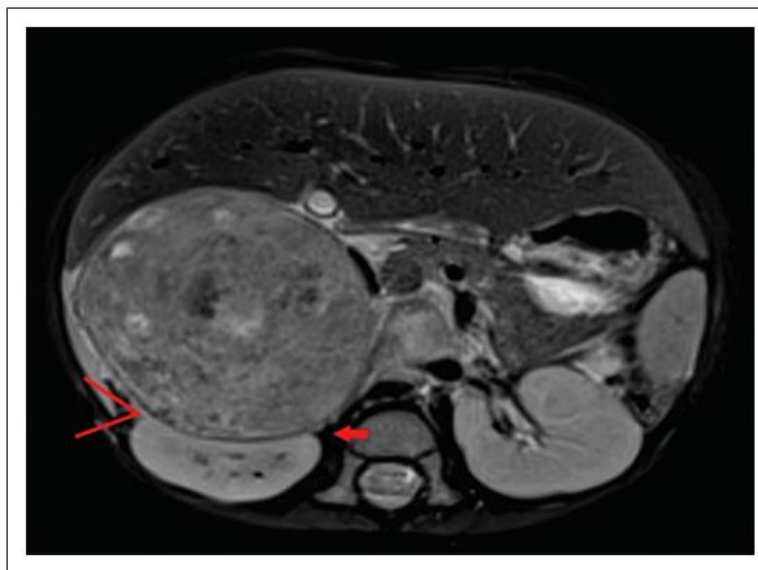


FIGURE 4: Axial fat-suppressed T2-weighted magnetic resonance image of a neuroblastoma compressing the right kidney. The claw sign is negative with absent tapering, infolding (red arrow) and acute external kidney–tumour interface.

Concerning the sample size, there were limitations. To maximize the research population, every attempt was taken to gather

comprehensive findings. However, instances were disqualified from the research if the requirements were not satisfied.

Unquestionably, as will be further described with respect to Cohen's kappa analysis, a bigger research sample would provide more precise and comprehensive findings. The frequentist approach contends that the underlying

statistical issue is also the most urgent. Cohen's kappa coefficients and their related CIs are based on a number of assumptions, many of which are questioned in light of the small sample size (53 instances).

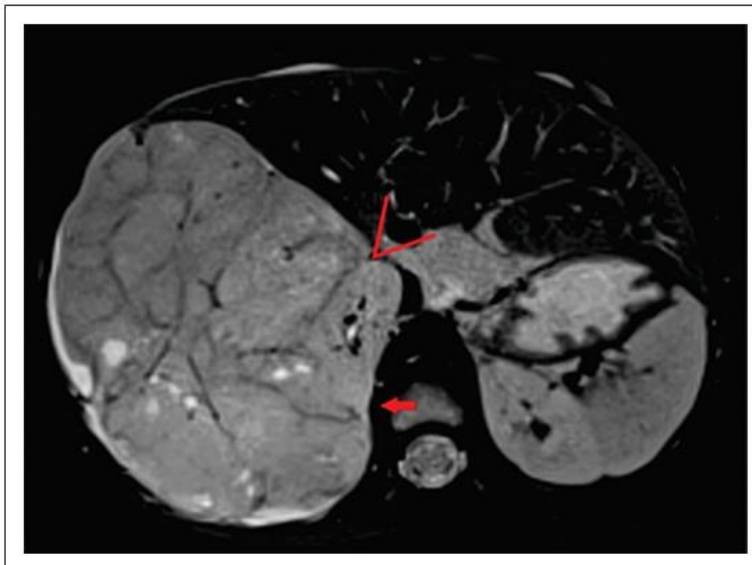


FIGURE 5: Axial fat-suppressed T2-weighted magnetic resonance image of a large nephroblastoma arising from the inferior pole of right kidney. The claw sign is positive at the posterior kidney–tumour interface (red arrow). However, there is infolding and an acute angle at the anterior kidney–tumour interface (red marker). In conflicting cases, a positive claw sign was diagnosed.

The comparison to inter-rater reliability with regard to the alleged "random" possibility of agreement among the two interpreters raises questions about Cohen's kappa analysis in particular (radiologists). (19) It is important to take into account the potential that comparing the level of agreement between two skilled specialists making a diagnosis within their area of specialization to a fully random probability may not be entirely accurate. When two physicians use the same set of abilities on the same issue, there should be some degree of agreement. The restricted number of inter-rater parties that may be evaluated using Cohen's kappa coefficient is another typical issue. (20)

CONCLUSIONS:The term "claw sign" refers to a mass with a distinctively tapered kidney edge, which may be corroborated by the absence of kidney edge infoldings and an acute external kidney-tumor contact. It hasn't been established that either the axial or coronal MRI

planes are preferable for assessing the sign. All the aforementioned traits and the overall perception of the claw sign have moderate to good intra- and inter-rater reliability. Although the claw sign lacks specificity, it is very sensitive. It was not possible to determine the tumor volume at which the claw sign operates most effectively. In-depth research is required to evaluate this.

REFERENCES:

1. Gbadamosi, H., Mensah, Y. B., Appau, A. A., & Renner, L. A. (2022). A spectrum of findings on computed tomography in paediatric abdominal and pelvic tumours in a Ghanaian teaching hospital. *Ghana Medical Journal*, 56(4), 295-302.
2. van der Beek, J. N., Artunduaga, M., Schenk, J. P., Eklund, M. J., Smith, E. A., Lederman, H. M., ... & Khanna, G. (2022). Similarities and controversies in imaging of pediatric renal tumors: A SIOP-RTSG and COG



- collaboration. *Pediatric Blood & Cancer*, e30080.
3. Bondera, T., Schubert, P., van Zyl, A., Pitcher, R., & Bagadia, A. (2022). Diagnostic yield and accuracy of paediatric image-guided fine needle aspiration biopsy of deep organ tumours. *SA Journal of Radiology*, 26(1), 1-9.
 4. Garg, A., & Swarup, M. S. (2022). Imaging Studies. In *Wilms' Tumor* (pp. 83-99). Springer, Singapore.
 5. Kim, H. H., Hull, N. C., Lee, E. Y., & Phillips, G. S. (2022). Pediatric Abdominal Masses: Imaging Guidelines and Recommendations. *Radiologic Clinics*, 60(1), 113-129.
 6. Elmalik, K., & Davies, B. (2022). Diagnostic Biopsy. *Wilms' Tumor*, 101-108.
 7. Yokota, H., & Tali, E. T. (2022). Spinal Infections. *Neuroimaging Clinics*, 33(1), 167-183.
 8. Julson, J. R., Noor, M. S., Williams, A. P., Wicker, J., & Beierle, E. A. (2022). A pediatric case of xanthogranulomatous pyelonephritis in the setting of Covid-19 and multi-system inflammatory syndrome (MIS-C). *Journal of Pediatric Surgery Case Reports*, 84, 102359.
 9. Bălănescu, R. N., Băetu, A. E., Moga, A. A., & Bălănescu, L. (2022). Role of Ultrasonography in the Diagnosis of Wilms' Tumour. *Children*, 9(8), 1252.
 10. Abib, S. D. C. V., Chui, C. H., Cox, S., Abdelhafeez, A. H., Fernandez-Pineda, I., Elgandy, A., ... & Gerstle, J. T. (2022). International Society of Paediatric Surgical Oncology (IPSO) Surgical Practice Guidelines. *ecancermedicalscience*, 16.
 11. Chandramohan, A., Bhat, T. A., John, R., & Simon, B. (2020). Multimodality imaging review of complex pelvic lesions in female pelvis. *The British Journal of Radiology*, 93(1116), 20200489.
 12. Figueroa, V. H., & Lorenzo, A. J. (2018). Surgical Approaches for Pediatric and Adolescent Renal Tumors. In *The Kelalis-King-Belman* (pp. 548-561). CRC Press.
 13. Roberts, S. B., Calligeros, K., & Tsirikos, A. I. (2019). Evaluation and management of paediatric and adolescent back pain: Epidemiology, presentation, investigation, and clinical management: A narrative review. *Journal of Back and Musculoskeletal Rehabilitation*, 32(6), 955-988.
 14. Adams, N. C., Farrell, T. P., O'shea, A., O'Hare, A., Thornton, J., Power, S., ... & Looby, S. (2018). Neuroimaging of central diabetes insipidus—when, how and findings. *Neuroradiology*, 60(10), 995-1012.
 15. Davis, J., Novotny, N., Macknis, J., Alpay-Savasan, Z., & Goncalves, L. F. (2017). Diagnosis of neonatal neuroblastoma with postmortem magnetic resonance imaging. *Radiology Case Reports*, 12(1), 191-195.
 16. Krishna, S., Schieda, N., Flood, T. A., Shanbhogue, A. K., Ramanathan, S., & Siegelman, E. (2018). Magnetic resonance imaging (MRI) of the renal sinus. *Abdominal Radiology*, 43(11), 3082-3100.
 17. Grover, S. B., Antil, N., Rajani, H., Grover, H., Kumar, R., Mandal, A. K., ... & Katyan, A. (2019). Approach to pediatric renal tumors: an imaging review. *Abdominal Radiology*, 44(2), 619-641.
 18. BujPradilla, M. J., MartíBallesté, T., Torra, R., & VillacampaAubá, F. (2017). Recommendations for imaging-based diagnosis and management of renal angiomyolipoma associated with tuberous sclerosis complex. *Clinical kidney journal*, 10(6), 728-737.
 19. Brillantino, C., Rossi, E., Minelli, R., Bignardi, E., Coppola, M., & Zeccolini, R. (2019). Current role of imaging in the management of children with Wilms Tumor according to the new umbrella protocol. *Transl Med*, 8, 1-16.
 20. Figueroa, V. H., & Lorenzo, A. J. (2018). Surgical Approaches for Pediatric and Adolescent Renal Tumors. In *The Kelalis-King-Belman* (pp. 548-561). CRC Press.

